Semiflexible Polymer Network: A View From Inside

A. Caspi, M. Elbaum,* R. Granek, A. Lachish, and D. Zbaida

Department of Materials and Interfaces, Weizmann Institute of Science, Rehovot 76100, Israel

(Received 19 August 1997)

The dynamics of a polymer network are studied by direct view observation of the motion of a single point within a single polymer. Taking advantage of rather rigid biological microtubules as a case study, we expand the space and time scales of the system to those accessible by optical microscopy and standard video tools. Tracking is achieved by chemically attaching an optically resolved microsphere to a single point on the filament. We study the time dynamics of this point, without spatial averaging inherent in scattering methods. It is shown that the mean square displacement of the individual point is sensitive to local filament and network properties. [S0031-9007(97)05158-2]

PACS numbers: 83.10.Nn

An essential physical question in the study of polymer dynamics is how to relate the bulk rheological response of a network to the molecular-scale motions executed by an individual monomer. The latter are driven by random thermal collisions with the surrounding solvent molecules, and constrained at two levels: the embedding of the monomer within the polymer and the entanglement of the polymer within the network. In conventional chemical polymers the relevant length scales are on the order of 1 nm, far too small to be resolved by direct imaging techniques. Typical methods of study include light and neutron scattering, which are sensitive to local fluctuations in the density of the bulk sample. Light scattering can provide superb time resolution, while the few-angstrom wavelength of neutrons offers much improved spatial sensitivity. Nonetheless, these methods make a spatial averaging of the fluctuations taking place in a large volume of the sample. Attention is typically focused on the time domain, with use of fluctuation-dissipation arguments to relate modes of response to the thermally generated fluctuations.

Recently, there have been a number of attempts to investigate local dynamics by direct imaging methods. The main trend has been to exploit biological polymers for their relative stiffness compared to simple synthetic ones, and also for their intrinsic biophysical interest. One approach has been to fluorescently label an entire polymer and watch its motion using video microscopy. The polymer is analyzed by measuring the wave vector [1] or the cosine correlation function [2]. In these methods the dynamics of a monomer is studied implicitly by measuring the dynamics of the entire polymer. Another method has been to implant a large bead in a network and investigate its restricted diffusion due to collisions with the surrounding filaments [3]. In this method, interpretation in terms of single filament dynamics must involve some *a priori* assumption.

The approach described here is to prepare a system in which it is possible to image monomer motion directly, and to study the polymer network via the dynamics of a single monomer [4]. To this end, we expand the size and time scales of the system by exploiting biological polymers known as microtubules. These self-assembling filaments are stiff enough to maintain an average direction from end to end, yet sufficiently flexible to display thermally driven undulations. We "tag" a single monomer by attaching to it an optically resolvable bead (Fig. 1) and trace the bead's position by video analysis. The motion of the bead displays the thermally driven motion of the microtubule itself. Using the clock provided by the video frame rate, we measure the mean square displacement (MSD) vs time interval of the bead. Classical random walk diffusion predicts that the MSD grows linearly in time, and our results lie in the deviations from this familiar situation. We interpret the data to probe the internal state of the network, e.g., to detect entanglement or quenched stress.

Background for this experiment is set by considering a bead attached to a single microtubule whose dynamics are governed by thermally driven bending fluctuations. The important parameters governing the MSD at a point

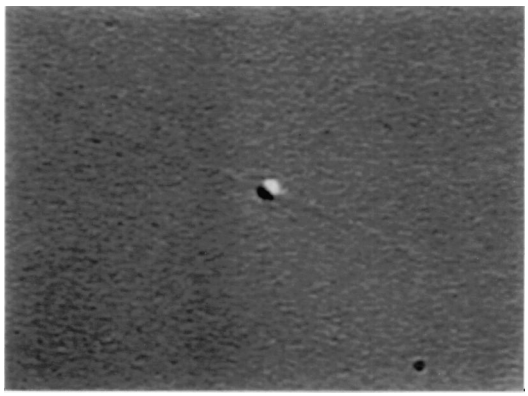

FIG. 1. Differential interference contrast image of a 0.3 μm bead attached to a single microtubule. The microtubule has a 25 nm diameter. A section appears as a diffraction-limited line when it lies in the plane of focus. The use of DIC optics allows the simultaneous observation of beads and microtubules. The horizontal dimension of the figure is 23 μm.

 0031-9007/98/80(5)/1106(4)$15.00

are the polymer length L and the persistence length L_p, on which scale thermal undulations decorrelate the tangent vectors of distant segments along the filament. The persistence length is defined as the ratio of the bending rigidity of the filament κ to the thermal energy k_BT ($L_p = \kappa/k_BT$). For microtubules, measurements by various techniques [5–7] yield L_p on the order of 2–10 mm. Since $L_p \gg L$, it is possible to define an average direction. The amplitude of fluctuations away from it are determined by the equipartition of thermal energy into all possible bending modes. The MSD of a point at a distance x along the baseline of the filament,

$$\langle \Delta h^2(x,t) \rangle = \langle [h(x,t) - h(x,0)]^2 \rangle , \quad (1)$$

is a measure of the ensemble average dynamics of the undulation amplitude $h(x,t)$ at this point. Using fixed end boundary conditions, it is given by the sum over bending modes from $n = 1$ to $n = L/a$ (n is the mode number and a is the filament diameter) [8,9]:

$$\langle \Delta h^2(x,t) \rangle = \frac{4}{L} \sum_{n=1}^{L/a} \frac{k_BT}{\kappa q^4} (1 - e^{-w(q)t}) \sin^2(qx) , \quad (2)$$

where $q = n\pi/L$ is the wave number of each excited mode and $k_BT/\kappa q^4$ is its contribution to the MSD resulting from the bending energy. The relaxation rate $w(q)$ of mode q, to leading order in qa, is given by

$$w(q) \approx \frac{\kappa q^4}{4\pi\eta} \ln(1/qa) , \quad (3)$$

where η is the solvent viscosity.

We consider two important limits. First, at short times, Eq. (1) reduces to

$$\langle \Delta h^2(x,t) \rangle \propto \frac{k_BT}{\eta^{3/4}\kappa^{1/4}} t^{3/4} \quad (4)$$

(full result in Ref. [10]). We see that in this regime the transverse motion at point x is *subdiffusive* with a power of $\frac{3}{4}$. Note that the prefactor is strongly dependent on κ (i.e., L_p) and effectively independent of L, and that there is no dependence on the position along the filament. In this short time regime the monomer does not feel the finite length of the polymer. Second, at long times, the amplitude of undulations comes to saturation,

$$\langle \Delta h^2(x,t) \rangle = \frac{2}{3} \chi^2 (1 - \chi)^2 \frac{L^3}{L_p} , \quad (5)$$

where $\chi = x/L$. As can be seen, the MSD saturation amplitude has a strong dependence on L; the monomer feels the entire length of the polymer. The crossover between the subdiffusion and saturation regimes takes place at a characteristic time τ_S, which is the inverse of the first mode relaxation rate $[w^{-1}(\pi/L)]$,

$$\tau_S = \frac{4}{\pi^3} \frac{\eta L^4}{\kappa \ln(L/\pi a)} . \quad (6)$$

Within a network of microtubules, the rotations, translations, and free undulations of individual filaments are constrained by distant entanglements [11]. From the point of view of the MSD at a point, this suppresses long wavelength undulations and effectively divides the microtubules into segments shorter than the physical length. It must also introduce some ambiguity to the boundary conditions applicable to each segment.

In this experiment we attach a bead to a microtubule to act as a neutral tracer. Of course, the presence of a bead of finite size alters the local motion of the polymer. We estimate this effect by writing the total friction force on the bead as a sum of the viscous friction $6\pi\eta R$ (R is the bead radius), which leads to the Stokes force, and an effective time dependent friction $\mu_e(t)$ due to constraining the bead to the polymer. The latter is estimated using Eq. (4) and the generalized Einstein relation $k_BT/\mu_e(t) = \langle \Delta h^2(t) \rangle/2t$. We find that only at time scales much shorter than those of our measurements is the behavior dominated by the Stokes force on the bead. For the measurable time scales the effect of the bead size is negligible, and the motion of the bead accurately reflects the motion of the bare microtubule to which it is attached.

Microtubules were purified from bovine brain as described in the literature [12]. They are a convenient material because they polymerize reversibly near room temperature, and their phase diagram is well established [13]. Structurally, they form hollow cylinders of 25 nm outer diameter and lengths up to hundreds of microns.

All observations were made by Nomarski differential interference contrast (DIC) microscopy (Zeiss optics, Fluar objective 100×, N.A. 1.3) and a digitally enhanced $\frac{1}{2}$ in. CCD camera (iSight iSC 2050LL), with a final resolution of 80 nm per pixel. The microtubule can be seen as a diffraction-limited line using the DIC microscope. The sample cell consisted of a long cover slip (22 × 40 mm, No. 1 thickness) fixed crosswise to an ordinary glass microscope slide (25 × 76 mm) using Parafilm spacers, leaving final dimensions approximately 5 × 25 × 0.1 mm. For each experiment, a solution of cold depolymerized tubulin [14] was injected to fill the cell. The sample was incubated at 30 °C for at least 30 min, during which time a network of microtubules developed. Beads were then injected from one side, and the cell was sealed. The area of observation was maintained at 30 °C, unless otherwise specified, by electrically heating the oil-coupled objective. The beads were silica microspheres, 0.3 μm diameter with carboxylate surface functionalization, reacted with tris solution so as to adhere to the microtubules via multiple hydrogen bonds [15]. Adhesion was verified by dragging the beads with optical tweezers based on an 830 nm single-mode laser diode. The tweezers could stretch or buckle the microtubules via the beads, showing that they attached to a single point and could not roll or slide.

The observation consisted simply of recording the bead motion, typically for 2–3 min (several thousand frames). A small region of interest surrounding a single bead was captured at a frequency up to the video frame rate (25 Hz)

into the disk of a personal computer. A "mask" image was taken of the bead itself, and then a correlation algorithm (MATROX INSPECTOR software) run in order to locate the position of the bead to a precision of $\frac{1}{4}$ pixel. The raw data is thus a list of (x_i, y_i) coordinates for the projection of the bead, and a corresponding counter specifying the frame number $i = 1, 2, \ldots, N$. The original (x_i, y_i) list was then rotated in small steps and the process repeated so as to align the measurement to the transverse and longitudinal axes of the microtubule. Data presented here come only from the transverse motion. Because the process is stationary, the MSD can be computed as a time average for a single trajectory, rather than an ensemble average. The analysis was cut off at long times when the data became too sparse to yield a statistically significant average [16]. Extraction of exponents from these calculations was made only on short times, typically 2–3 sec. Account was also taken of missed frames in the video capture and image location functions. In order to test our methods, we applied this technique to a sample of beads in a sucrose solution (33% by weight). For that known case, we measured an ordinary diffusion $\langle \Delta h^2(t) \rangle \sim t^{\gamma}$ with a power $\gamma = 1.00 \pm 0.02$.

Results from three exemplary cases are shown in Fig. 2. Note the common qualitative features of a subdiffusion regime at short times, where $\langle \Delta h^2(t) \rangle \sim t^{\gamma}$ with a power $\gamma < 1$. From 20 measurements we have an average exponent $\gamma = 0.75$, with a standard deviation of 0.04. For longer times we can distinguish cases that display a saturation (curves *A* and *B*) from those that do not (curve *C*). The saturation itself shows different characteristic time and amplitude in each measurement, corresponding to different local entanglement lengths [17] in the polymer network. The cases where we did not observe a saturation regime belong to measurements taken in sparse networks, usually at lower temperature (25 °C). In these cases, only 3–4 filaments typically appeared in a field of view, while more than 20 filaments appeared in the cases where we observed saturation in the time scale of the measurements. In order to observe saturation, the crossover time τ_S must be on the order of 1 sec. Inverting Eq. (6), this corresponds to a length of 30 μm, while the physical length of the microtubules was typically much longer than 100 μm. We conclude from this that the presence of an observable saturation regime is a result of the network, in which the filaments are divided into effectively shorter segments by constraints at distant entanglement points.

The results shown in Fig. 3 belong to cases where the saturation time is very long and we see only the short time behavior of the polymer undulation. The triangular points are of the frequent case of a sparse network. Dragging the fibers by pulling on the bead with the optical tweezers caused them to bend or stretch, showing that they were nonetheless entangled at some length. Here, as in curve *C* in Fig. 2, the undulation dominated behavior with $\gamma = 0.75$ continues to the longest observation times. Substituting the measured prefactor from the power-law fit into Eq. (4) gives a persistence length of $L_p \approx 7$ mm. However, the fourth power in the equation makes this type of measurement of L_p overly sensitive to small errors.

Two salient exceptions from the typical behavior also appear in Fig. 3. In the upper curve, plotted in circles, a short polymer floats freely without entanglements. Bending fluctuations are superimposed upon, but indistinguishable from, the translational diffusion. Dragging the bead using the optical tweezers did not induce bending of the

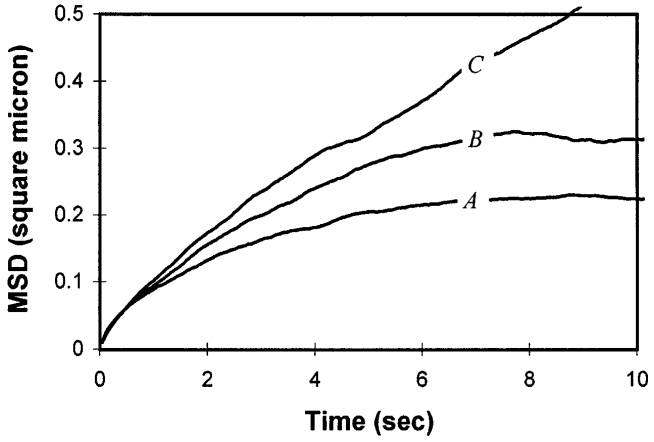

FIG. 2. Measured results of the transverse MSD of a 0.3 μm bead attached to a point on a microtubule filament. Three exemplary cases are shown. Curves *A* and *B* show a saturation regime.

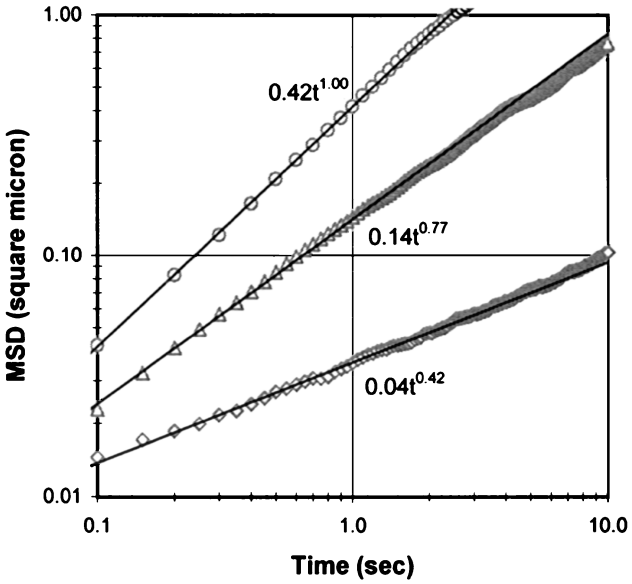

FIG. 3. Logarithmic presentation of MSD data for monomer dynamics in three different network types. Triangles: the frequent case of undulation with a power law of $\frac{3}{4}$. Circles: a free filament with ordinary diffusion; the undulation dominated regime would be apparent only at much shorter times. Diamonds: a prestressed network. The full line in each graph is a power-law fit which was calculated on a time interval less than 3 sec.

polymer. The MSD result, to within our time resolution imposed by the video capture rate, is an ordinary diffusion exponent, $\gamma = 1$. No distinction was observed between transverse and longitudinal motions. The derived diffusion constant is consistent with a rod of length 40 μm, which coincides with the observed length in this unusual case. The ordinary diffusion implies that the undulation dominated regime, $\gamma = 0.75$, is pushed to shorter times. Indeed, comparing the MSD expected due to the thermal undulations to that of a freely diffusing rod with length 40 μm, we find that diffusion dominates at times longer than 0.05 sec.

The lower curve in Fig. 3, marked by diamonds, displays MSD results from a sample prepared in a peculiar way. Instead of injecting cold, depolymerized tubulin to the sample chamber, the microtubule network was polymerized in a test tube with the beads and then injected fully formed. This led to a twisted, stressed network because many of the microtubules were already longer than the smallest dimension of the chamber. Note that the measured subdiffusion exponent becomes $\gamma = 0.42$. Interpretaton of the smaller exponent can be made if we assume that, in deforming the network, entangled polymer segments are put in tension. The relevant analogs to Eqs. (2) and (3) are obtained by replacing the term κq^4 with $(\kappa q^4 + \sigma q^2)$, where σ is the tension along the polymer. It can be shown [9] that, at times where $4\pi\eta\kappa/\sigma^2 \ll t \ll \eta L^2/\sigma$, the MSD becomes

$$\langle \Delta h^2(t) \rangle \propto \frac{k_B T}{(\sigma\eta)^{1/2}}\, t^{1/2}\,. \qquad (7)$$

Note the smaller subdiffusion exponent of the undulation, $\gamma = \frac{1}{2}$, in the case of tension along the polymer.

A similar exponent ($\gamma = 0.4$–0.5) is also found when we use the optical tweezers to introduce tension in the filament. This was done using microtubules to which two beads were attached at some distance. The MSD measurement was made on one bead while the other was pulled into the trap of the optical tweezers. Releasing the trapped bead caused a return to the typical exponent $\gamma = 0.75$.

In summary, we report experimental measurements of single monomer dynamics. The motion of this point is sensitive to the nature of the polymer network in which it is embedded. Our measurements extend to sufficiently long times to observe a saturated regime of the undulation, as a consequence of entanglements along the filament. At short times, we measure directly the anomalous diffusion with power law $\frac{3}{4}$ due to thermally driven undulations of a single polymer. The latter result supports the conclusions of earlier works by less direct methods [3,8,18]. In addition, we find a subdiffusive regime with power law 0.4–0.5 for a deformed network, interpreted as a signature of tension along the individual filament. The direct view on a single point avoids spatial averaging and thus permits observation of exceptional cases, even when they do not dominate the sample.

We wish to thank J.-P. Munch, J. Prost, and A. G. Zilman for discussions of background and motivation, and J. S. Wettlaufer for a critical review of the manuscript. This work was supported in part by NASA, Microgravity Materials Science Program, Contract No. NAG8-1277. R. G. would like to thank the Israel Science Foundation for support.

*Author to whom correspondence should be addressed.

[1] J. Käs, H. Strey, M. Bärmann, and E. Sackmann, Europhys. Lett. **21**, 865 (1993).
[2] A. Ott, M. Magnasco, A. Simon, and A. Libchaber, Phys. Rev. E **48**, R1642 (1993).
[3] F. Amblard, A. C. Maggs, B. Yurke, A. N. Pargellis, and S. Leibler, Phys. Rev. Lett. **77**, 4470 (1996).
[4] By "monomer" we mean the elementary chemical repeat unit of the polymer.
[5] F. Gittes, B. Mickey, J. Nettleton, and J. Howard, J. Cell Biol. **120**, 923 (1993).
[6] H. Felgner, R. Frank, and M. Schliwa, J. Cell. Sci. **109**, 509 (1996).
[7] M. Elbaum, D. K. Fygenson, and A. Libchaber, Phys. Rev. Lett. **76**, 4078 (1996).
[8] E. Farge and A. C. Maggs, Macromolecules **26**, 5041 (1993).
[9] R. Granek, J. Phys. II (France) **7**, 1761 (1997).
[10] The MSD of the monomer at short times is [9]

$$\langle \Delta h^2(x,t) \rangle = 0.041\left[\ln\left(\frac{\kappa t \ln(L/\pi a)}{4\pi\eta a^4}\right)\right]^{3/4} \times \left(\frac{k_B T}{\eta}\right)^{3/4} \frac{1}{L_P^{1/4}}\, t^{3/4}\,.$$

[11] M. Doi, J. Phys. (France) **36**, 607 (1975).
[12] K. L. Carraway and C. A. C. Carraway, *The Cytoskeleton* (Oxford Press, New York, 1992).
[13] D. K. Fygenson, E. Braun, and A. Libchaber, Phys. Rev. E **50**, 1579 (1994).
[14] Tubulin solution is prepared at 35 μM concentration, plus GTP 1 mM in PME buffer: Pipes 100 mM, pH 6.9, $MgCl_2$ 2 mM, and EGTA 1 mM.
[15] Carboxylated silica beads 0.3 μm diameter, from Bangs labs (3 μl, 10% solids) were gently mixed with tris [hydroxymethyl] aminomethane solution (50 mg/0.5 ml) for 2 h at room temperature. The beads were washed three times with 0.5 ml distilled water and suspended in 1 ml PME buffer plus GTP 1 mM.
[16] H. Qian, M. P. Sheetz, and E. L. Elson, Biophys. J. **60**, 910 (1991).
[17] We define the entanglement length as the distance between consecutive entanglements along the filament.
[18] C. F. Schmidt, M. Bärmann, G. Isenberg, and E. Sackmann, Macromolecules **22**, 3638 (1993).